DocID: https://connectjournals.com/03896.2020.20.5101

Biochem. Cell. Arch. Vol. 20, No. 2, pp. 5101-5105, 2020 | www.connectjournals.com/bca | *ISSN 0972-5075*

CYTOTOXICITY OF IRON DOPED SULFATED ZIRCONIA NANOPARTICLES: SYNTHESIS, CHARACTERIZATION AND *IN VITRO* STUDY

Qasim Khlaif Abdullah[1], Mohamed Qasim Al-Fahdawi[2], Ruaa Tareq Hammad[3], Eltayeb E. M. Eid[4], Mothanna Sadiq Al-Qubaisi[2] and Abdullah Rasedee[5*]

[1]Pediatric Department, Ramadi Teaching Hospital for Gynecology and Childhood, University of Anbar, Ramadi, Iraq.

[2]Institute of Bioscience, Universiti Putra Malaysia, 43400 UPM Serdang, Selangor, Malaysia.

[3]Department of Chemistry, Faculty of Science, University of Anbar, Ramadi, Iraq.

[4]Department of Pharmaceutical Chemistry and Pharmacognosy, Unaizah College of Pharmacy, Qassim University, Saudi Arabia.

[5]Department of Veterinary Pathology and Microbiology, Faculty of Veterinary Medicine, Universiti Putra Malaysia, 43400 UPM Serdang, Selangor, Malaysia

*Corresponding author e-mail: rasedee@upm.edu.my

(Received 11 June 2020, Revised 30 September 2020, Accepted 3 October 2020)

ABSTRACT : Nanostructured iron-doped sulfated zirconia was prepared via the precipitation and dry spray technique followed by calcination at 700°C for 5h. The physicochemical characterization of these nanomaterials was performed using X-ray diffraction, X-ray photoelectron spectroscopy and transmission electron microscopy. The average diameter of iron-doped sulfated zirconia nanoparticles is estimated to be 29/nm. The anti-cancer effects of iron-doped sulfated zirconia nanoparticles were examined on the human breast cancer MDA-MB-231, colon cancer HT29 and liver cancer HepG2 cell lines using the MTT (4,5-dimethylthiazol-2-yl)-2,5-diphenyltetrazolium bromide) assay. The study showed that iron-doped sulfated zirconia nanoparticles have potential to be developed into an anti-cancer compound.

Key words : Nanoparticles, X-ray photoelectron spectroscopy, anti-cancer.

INTRODUCTION

Transition metals and biomedical applications were once considered to be mutually exclusive. Metals were thought to be extremely poisonous and unstable in aqueous media. However, in 1965, with the discovery of cis-diamine-dichloro-platinum(II) (cisplatin) that has anticancer effects, came the realization that transition metal complexes in fact have medical applications. Since then, transition metal complexes have been used in radiation therapeutics, as diagnostic and imaging agents and in the development of small molecule drugs (Khomskii, 2014).

Zironiums have many medical applications. This transition metal binds to urea and it is currently used in the treatment of chronic kidney disease (Wolfe and Chang, 1987; Boschini *et al*, 2003). Sulphated zirconia and iron-manganese-doped sulfated zirconia nanoparticles were recently synthesized and these nanoparticles were shown to exhibit effective anti-proliferative and antimicrobial properties (Mftah *et al*, 2015; Al-Fahdawi *et al*, 2015). Sulfated zirconia nanoparticles are particularly promising as an antiproliferative compound for human breast cells since, it is relative harmless to the normal human breast cells (Mftah *et al*, 2015). Even with great potentials in medical applications, there is limited information on transition metal oxide nanoparticles as anti-cancer agents. This is a first study that reports the *in vitro* cytotoxic effect of iron-doped sulfated zirconia nanoparticle on human colon cancer HT29, breast cancer (MDA-MB-231) and liver cancer (HepG2) cell lines.

MATERIALS AND METHODS

Iron-doped sulfated zirconia was prepared via the precipitation and hydrothermal impregnation method. 7.5 g of hydrated zirconyloxynitrate were dissolved in 200 mL deionized water with the dropwise addition of 30% ammonia until a white gelatinous precipitate was formed. The 30% ammonia solution maintained the pH of the suspension at 8 to 11. The precipitate was allowed to age for 24 h, filtered using a vacuum pump, washed with 600 mL of warm deionized water, and then dried at 120°C for approximately 18 h. Hydrated iron (iii) nitrate (0.60 g) and $(NH_4)_2\ SO_4$(1.150 g) were dissolved in 200 mL deionized water. The solution was added dropwise with vigorous stirring to the zirconium oxyhydroxide solution. The final solution, while vigorously stirred, was left at ambient temperature for 6 h before placing ina closed autoclave reactor to dehydrate at 150°C for 24h. Calcination of the product was done at 700°C for 5h.

The X-ray photoelectron spectroscopy(XPS) data were obtained using modified photoelectron spectrometry

(Kratos Analytical, Shimadzu Corporation, Japan), furnished with a hemispherical analyser at an excitation, radiation of AlKα (1486.6 eV). The analysis was done at a transmission mode of 40 electron volts pass energy. The X-ray gun was activated at 4 mA emission current with stepping up of voltage 15 kilovolts. Samples were pre-treated under a vacuum (1×10^{-9} Torr) at 22 ± 2° for 2 h before analysis. The analyzer chamber was under base pressure of 1×10^{-9} Torr. During the data collection, the pressure was constantly at $< 1 \times 10^{-9}$ Torr. The electron binding energy (BE), relative to C 1s peak and taken as 284.5 eV was determined for C 1s, Zr 3d, Fe 2p, Mn 2p, S 2p and O 1s.

The X-ray diffraction (XRD) characterization of nanoparticle powder was performed using the Shimadzu diffractometer model XRD 6000, Japan. The diffraction pattern of the powdered samples was obtained with the Cu-K_α radiation generated at ambient temperature.

Transmission electron microscopy (TEM) (Hitachi H-7100, Japan) was used to determine the fine structure of the nanoparticles crystals. The nanoparticle powder disseminated in deionized water was placed onto carbon-cover copper grids on filter paper and dried at room temperature before viewing.

The cell lines used in the cytotoxicity study of our nanoparticleswere human breast adenocarcinoma (MDA-MB-231), human colorectal adenocarcinoma (HT29), human hepatocellular carcinoma (HepG2), human umbilical vein epithelial cell (HUVEC) and normal human liver (Chang) cells [American Type Culture Collection (ATCC; Rockville, MD, USA)]. MTT (3-(4,5-dimethylthiazol-2-yl)-2,5-Diphenyltetrazolium Bromide; Sigma-Aldrich, St. Louis, MO, USA) assay was done at 37°C for 72 h as previously described (Al-Fahdawi *et al*, 2015).

RESULTS AND DISCUSSION

Fig. 1 shows the X-ray photoelectron spectra of nanoparticles. The iron-doped sulfated zirconia is represented by the photoelectron peaks at 181.0 and 530.3 eV ascribed to zirconium 3d5/2 and O1s orbitals, respectively. Both photoelectron lines are due to zirconium oxide (Scheithauer *et al*, 1998). The higher binding energy of 185.2 eV corresponds to the growth of Zr^{+4} involving electronegative anions. The lack of the effect on the profile of the zirconium 3d orbital line is a very important finding because it suggests there are interactions at the interfaces of sulfate anion and zirconium oxide for $(NH_4)_2 SO_4$ during the hydrothermal impregnation. The S2p photoemission peaks are located at approximately 167.9 eV (Fig. 1-iii), showing the occurrence of sulfur (+6) that is comparable with the S^{+6} in sulfate species (Wu *et al*, 2013). Fig. 1-iv displays the XPS spectrum of nanoparticle in the zone of iron 2p. The iron 2p3/2 and 2p1/2 emission lines appeared at approximately 710.3 and 724.2 eV, respectively and these are evidences for the presence of iron oxide on the surface of the iron-doped sulfated zirconia. Furthermore, the photoelectron profile is a confirmation for the occurrence of iron ions that are almost comparable with the iron oxide photo-emission

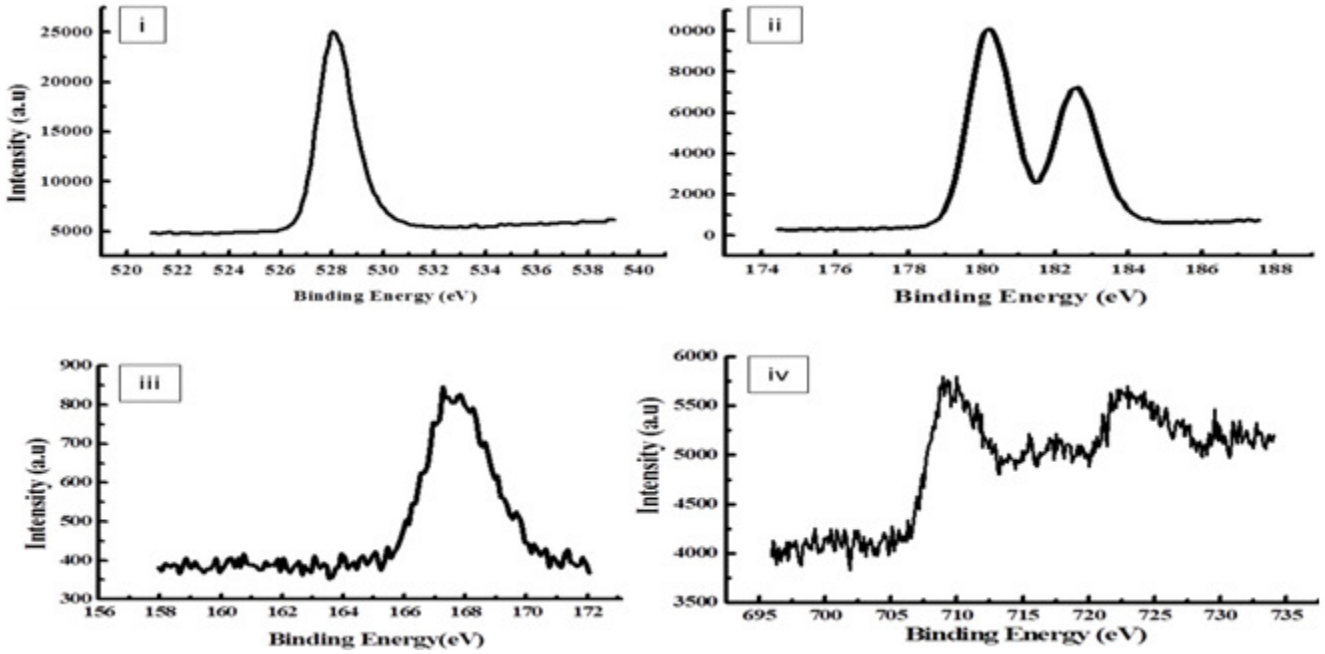

Fig. 1 : X-ray photoelectron profiles of iron-doped sulfated zirconia nanoparticles. (i) O-2 Is; (ii) Zr4+ 3d5/2; (iii) Fe3+ (2p3/2, 2p1/2); (iv) S6+ 2p.

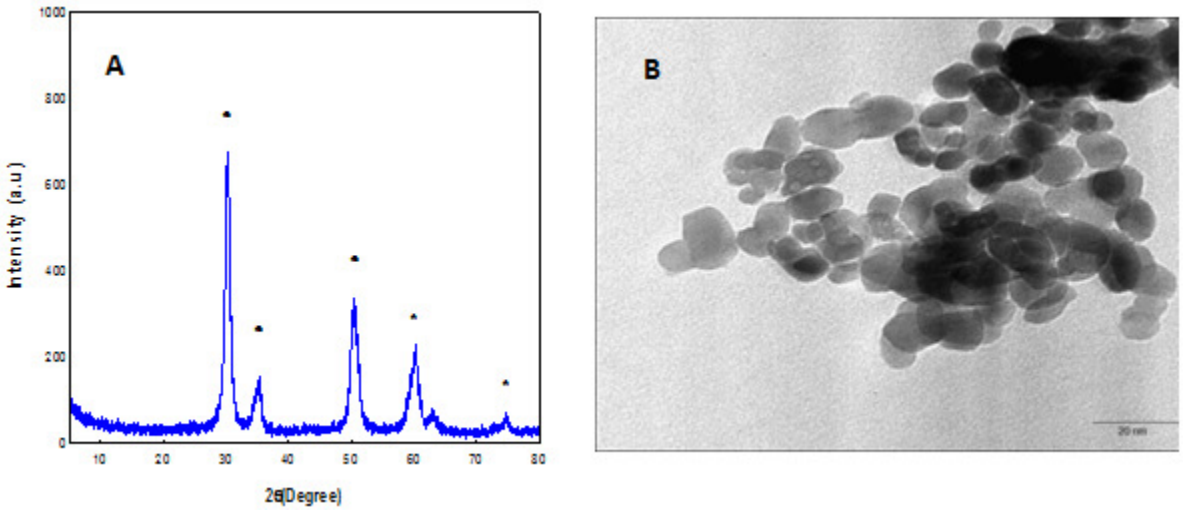

Fig. 2 : A) XRD pattern of iron-doped sulfated zirconia sample calcined at 700 °C for 5h. (♣) tetragonal phase of zirconia. **B)** Transmission electron microscopic image of nanoparticles calcined at 700 °C for 5h.

lines (Alhassan *et al*, 2014).

Fig. 2. A depicts X-ray diffraction patterns of the iron-doped sulfated zirconia nanoparticles that consisted of only the tetragonal zirconia phase at 2λ = 30.27°, 34.8°, 50.4° and 60.2° (JSPDS file No: 00-050-10589-Zirconium oxide) (Yamamoto *et al*, 1999). Nonetheless, the diffraction peaks confirmed that the absence of monoclinic phase in the nanoparticles, indicating the tetragonal phase stability of the crystalline structure. The absence of the iron oxide diffraction peaks suggests that the iron oxide was well distributed on the ZrO_2 surface. The dispersion of iron oxide nanoparticles in fact improved the stability of the tetragonal phase and produced higher BET surface area (Garvie and Goss, 1986). The size of the Fe^{3+}-SO_4/ZrO_2 (iron-doped sulphated zirconia nanoparticles) crystals determined by the Debye-Scherrer's equation was 32.0 nm.

The nature of the crystal and the degree of dispersion of nanoparticles was also determined by TEM (Fig. 2B). The nanoparticle crystals are tetragonal with diameters between 26.2 to 31.8 nm with an average size of 28.9 nm. The zirconia nanoparticles areaggregated in appearance.

Nanoparticles showed greater cytotoxic effects toward the HepG2, HT29 and MDA-MB-231 than the HUVEC and Chang cell lines, (Table 1, Fig. 3). Comparatively, at 61.5 µL and after 72 h, the nanoparticles are more toxic to HepG2 and MDA-MB-231 than the HT29 cell lines, as suggested by their respective cell viability by 59, 51 and 19%, after the treatments. At the same concentration and treatment period, the nanoparticles was 3.7 times more toxic to HUVEC than Chang cells. Among cancer cell lines, nanoparticles showed the lowest 72 h $IC_{50}$of 30.9 µg/mL toward the HepG2 cells (Table 1).

Table 1 : IC_{50} values of iron-doped sulfated zirconia nanoparticles and drugs on cancer cells at 72 h.

Cells	Iron-doped sulfated zirconia nanoparticles (µg/mL)	(Drug) g/mL
HT29	172.77	3.59 (Oxaliplatin)
MDA-MB-231	61.52	0.27 (Doxorubicin)
HepG2	30.86	3.22 (Tamoxifen)
Chang	275.05	1.19 (Tamoxifen)
HUVEC	108.93	2.47 (Tamoxifen)

CONCLUSION

The iron-doped sulfated zirconia prepared via precipitation and hydrothermal impregnation exhibited aggregated tetragonal nanoparticles. These nanoparticles were significantly toxic to HepG2 and MDA-MB-231 cell lines and considerably less so toward the normal Chang and HUVEC cells. Among the cancer cell lines, the human colon cancer, HT29, cells showed the highest resistance to cytotoxic effect of nanoparticles. The study, for first time,showed that iron-doped sulfated zirconia nanoparticles can potentially be developed intoanti-cancer compound.

Conflict of interests

The authors report no conflicts of interest.

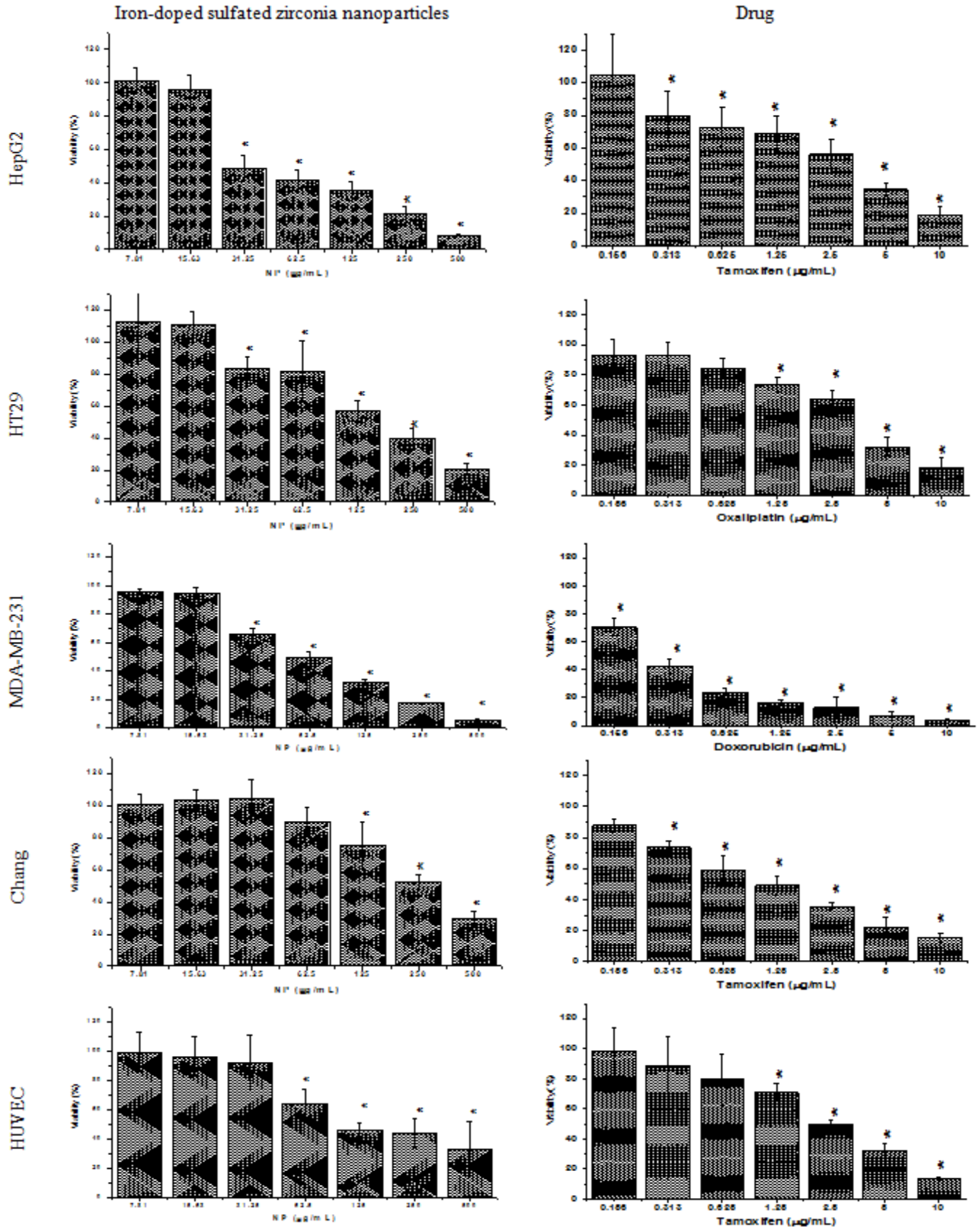

Fig. 3 : Iron-promoted sulfated zirconia NP and chemotherapeutic effects on the viability of treated cells, which were evaluated through mitochondrial activity using a 3-(4,5-dimethylthiazol-2-yl)-2,5-diphenyltetrazolium bromide assay.HepG2 = human heptacellular carcinoma cell line; HT29 = Human colorectal adenocarcinoma cell line; MDA-MB-231 = human breast adenocarcinoma; Chang cell = normal human liver cell line; HUVEC = human umbilical vein endothelial cell line. **Notes:** Mean ± standard deviation (n=9 wells/ treatment). *P<0.05 compared with the untreated cells.

REFERENCES

Al-Fahdawi M, Rasedee A, Alhassan F H, Al-Qubaisi M S, Rosli R, El Zowalaty M E, Sh-eldin M, Webster T J and Taufiq-Yap Y H (2015) Cyctotoxicity and physicochemical characterization of iron – manganese doped sulfated zirconia nanoparticles. *Int. J. Nanomedicine* **10**, 5739–5750. doi: 10.2147/IJN.S82586.

Alhassan F H, Rashid U, Yunus R, Sirat K, Ibrahim L M and Taufiq-Yap Y (2014) Synthesis of ferric–manganese doped tungstated zirconia nanoparticles as heterogeneous solid superacid catalyst for biodiesel production from waste cooking oil. *Int. J. Green Energy* **15**, 987-994. doi.org/10.1080/15435075.2014.880843.

Boschini F, Robertz B, Rulmont A and Cloots R (2003) Preparation of nanosized barium zirconate powder by thermal decomposition of urea in an aqueous solution containing barium and zirconium, and by calcination of the precipitate. *J. Europ. Ceramic Society* **23**(16), 3035-3042.

Garvie R and Goss M (1986) Intrinsic size dependence of the phase transformation temperature in zirconia microcrystals. *J. Materials Sci.* **21**(4), 1253-1257.

Khomskii D (2014) *Transition Metal Compounds*. Cambridge University Press, U.K.

Mftah A, Alhassan F H, Al-Qubaisi M S, El Zowalaty M E, Webster T J, Sh-eldin M, Rasedee A, Taufiq-Yap Y H and Rashid S S (2015) Physicochemical properties, cytotoxicity and antimicrobial activity of sulphated zirconia nanoparticles. *Int. J. Nanomedicine* **10**, 765.

Scheithauer M, Bosch E, Schubert U A, Knözinger H, Cheung T-K, Jentoft F C, Gates B C and Tesche B (1998) Spectroscopic and microscopic characterization of iron-and/or manganese-promoted sulfated zirconia. *J. Catalysis* **177**(1), 137-146.

Wolfe E and Chang T (1987) Orally ingested microencapsulated urease and an adsorbent, zirconium phosphate, to remove urea in kidney failure. *The Int. J. Artificial Organs* **10**(4), 269-274.

Wu Y, Qin L, Zhang G, Chen L, Guo X and Liu M (2013) Porous Solid Superacid SO42–/Fe2–x Zr x O3 Fenton Catalyst for Highly Effective Oxidation of X-3B under Visible Light. *Industrial & Engineer. Chem. Res.* **52**(47), 16698-16708.

Yamamoto T, Tanaka T, Takenaka S, Yoshida S, Onari T, Takahashi Y, Kosaka T, Hasegawa S and Kudo M (1999) Structural analysis of iron and manganese species in iron-and manganese-promoted sulfated zirconia. *The J. Physical Chem. B* **103**(13), 2385-2393.